Implications to Other Systems. Extension of the ideas presented here to other tripositive metal–oxalate complexes must be made with caution because of the unknown effect of the nature of the ligands on the photochemical processes. Thus, conclusions about the detailed behavior of $Co(C_2O_4)_3^{3-}$, for example, cannot be drawn by analogy to the amine–oxalate systems. We have already indicated, however, that the secondary formation of Co^{2+} in the photolysis of $Co(C_2O_4)_3^{3-}$ *via* reaction 9 is so rapid as to compete successfully with the removal of the radicals by O_2 in reaction 11. Only at low complex concentrations is the yield of Co^{2+} affected by the presence of O_2.[9] Thus, the assumption made in earlier work[5] that the quantum yield of primary Co^{2+} formation is one-half of the observed value of $\phi_{Co^{2+}}$ is correct. It is interesting to note that Cooper and DeGraff[47] obtained a rate constant of $>5 \times 10^7\ M^{-1}\ sec^{-1}$ for $C_2O_4^-/CO_2^- + Fe(C_2O_4)_3^{3-}$ from their flash photolysis study indicating a fast secondary formation of Fe^{2+}. They also obtained a long-lived intermediate absorbing at $\lambda < 460$ nm which they could only identify very tentativly. Future work on these and related systems will be directed toward answering the many questions raised by the study reported here.

(47) G. D. Cooper and B. A. DeGraff, *J. Phys. Chem.*, 75, 2897 (1971).

Summary

The ultraviolet photochemistry of the amine–oxalate complexes of Co(III), $(NH_3)_5Co(C_2O_4)^+$, $(NH_3)_4Co(C_2O_4)^+$, and $(en)_2Co(C_2O_4)^+$ generates, in addition to Co^{2+} and a radical derived from the one-electron oxidation of oxalate ($C_2O_4^-$, CO_2^- or their protonated analogs), excitation localized on the oxalate ligand. This "intramolecular sensitized" ligand excitation results in heterolytic C–C bond scission and leads to the formation of CO_2 and a C-bonded formato linkage isomer complex of Co(III). This C-bonded formato species is unstable with respect to Co^{2+} and undergoes thermal intramolecular electron transfer with a rate that is dependent upon the state of protonation of the formato ligand and the nature of the amine ligands. The production of Co^{2+} by this indirect route is accompanied by the generation of radicals (CO_2^- or CO_2H). The radicals formed here and in the primary direct production of Co^{2+} reattack and reduce the complex (except for the protonated radicals and the en complex) to generate a secondary source of Co^{2+}. The radicals can be scavenged by O_2 to reduce the value of $\phi_{Co^{2+}}$ by a factor of 2.

Acknowledgment. This research was supported by NSF Grant No. GP 11213. The authors wish to thank Professor J. N. Armor for assistance in the separation and characterization of en-LL and Dr. E. Rotlevi for help in obtaining some of the data on $(NH_3)_5Co(C_2O_4)^+$.

Photochemical Reaction Pathways of Ruthenium(II) Complexes. III.[1] Metal-to-Ligand Charge-Transfer Excitation of the Pentaamminepyridineruthenium(II) Cation and Related Species[2]

Donald A. Chaisson, Ray E. Hintze, Daniel H. Stuermer,[3a] John D. Petersen, Daniel P. McDonald, and Peter C. Ford*[3b]

Contribution from the Department of Chemistry, University of California, Santa Barbara, California 93106.

Received January 15, 1972

Abstract: Product analyses and quantum yields are reported for the photoreactions resulting from metal-to-ligand charge-transfer excitation of the complex ion $Ru(NH_3)_5py^{2+}$. Photoaquation of pyridine and of cis and trans ammonias are the principal reaction pathways. Quantum yields for pyridine photoaquation show an unusual dependence on solution pH plateauing at ~0.04 mol/einstein at high pH and appearing to level at ~0.12 mol/einstein for low pH (2.0 *M* ionic strength). Ammonia photoaquation is apparently pH insensitive. Quantum yields were also measured for the photoaquation of L from the complexes $Ru(NH_3)_5L^{2+}$ (L = benzonitrile, 3-chloropyridine, 4-methylpyridine). These were independent of pH for L = benzonitrile and for L = 3-chloropyridine except at very low pH's. In contrast, the quantum yields for L = 4-methylpyridine followed a pH pattern similar to that observed for L = pyridine. In the higher pH region, the Φ_L values followed the order L = benzonitrile > 3-chloropyridine > pyridine > 4-methylpyridine. Photolysis of $Ru(NH_3)_5py^{2+}$ in acidic D_2O gave small yields of H/D exchange on the pyridine ring. The quantum yield of this pathway, however, was too small to indicate a major role in the photoaquation. These data are interpreted in terms of proposed photoaquation mechanisms which for $Ru(NH_3)_5py^{2+}$ involve competitive protonation of an excited state or intermediate.

In recent years, there has been considerable interest in the mechanistic photochemistry of octahedral metal ammine complexes.[4–7] These studies have principally

(1) Papers I and II are respectively (a) P. C. Ford, D. H. Stuermer, and D. P. McDonald, *J. Amer. Chem. Soc.*, 91, 6209 (1969); (b) P. C. Ford, D. A. Chaisson, and D. H. Stuermer, *Chem. Commun.*, 530 (1971).

(2) Taken in part from the M.A. dissertation of D. A. C., University of California, Santa Barbara, 1971. This work has been presented in part at the 161st National Meeting of the American Chemical Society, Los Angeles, Calif., April 1971.

(3) (a) National Science Foundation Undergraduate Research Participant, summer 1969; (b) Camille and Henry Dreyfus Foundation Teacher–Scholar.

(4) For comprehensive reviews, see (a) V. Balzani and V. Carassiti, "Photochemistry of Coordination Compounds," Academic Press,

been concerned with excitation from two types of electronic transition: ligand field (d–d) absorptions and ligand-to-metal charge-transfer (LMCT) absorptions. Previously, we reported[1] the photoaquation pathways resulting from metal-to-ligand charge-transfer (MLCT) excitation of aqueous pentaamminepyridineruthenium(II), $Ru(NH_3)_5py^{2+}$, and the influence of pH on the quantum yields of these pathways. To our knowledge, those studies and the work presented here constitute the first systematic investigation of the photoreaction mechanisms of cationic ruthenium(II) ammine complexes and of pathways resulting from MLCT excitation of a metal ammine complex. A study of the MLCT photochemistry of the $Ru^{II}(NH_3)_5L$ complexes structurally and electronically (low spin $4d^6$) analogous to the other systems investigated [*e.g.*, Co(III) ($3d^6$), Rh(III) ($4d^6$), Pt(IV) ($5d^6$)] may provide insight into the interrelationships of electronic excitation and reaction modes.

Experimental Section

Materials. The recrystallized complex salts $[Ru(NH_3)_5L][BF_4]_2$ (L = pyridine, 3-chloropyridine, 4-methylpyridine, or benzonitrile) were prepared from $[Ru(NH_3)_5Cl]Cl_2$ by published procedures.[8,9] The deuterium oxide (Stohler Isotope Chemicals) and deuteriosulfuric acid (Ventron) of the pyridine deuteration studies were used without further purification. Water used for solutions was redistilled from alkaline permanganate. All reagents used to prepare photolysis solutions were reagent grade. Argon used for deaeration was deoxygenated by passage through Cr(II) solution in gas scrubbing bottles. Buffer solutions used in quantum yield determinations (0.2 *M* ionic strength) were prepared as follows: pH's 3.0 and below, HCl–NaCl, $[Cl^-] = 0.2$ *M*; pH 3.8, potassium biphthalate (0.10 *M*)–NaCl (0.10 *M*), pH adjusted with HCl; pH 4.6, acetic acid (0.10 *M*)–sodium acetate (0.10 *M*)–NaCl (0.10 *M*); pH 6.8, KH_2PO_4 (0.025 *M*)–Na_2HPO_4 (0.025 *M*)–NaCl (0.10 *M*); pH 8.1, HCl (0.10 *M*)–tris(hydroxymethyl)aminoethane (0.20 *M*)–NaCl (0.10 *M*); pH 9.2, NH_4Cl (0.10 *M*)–NH_3 (0.10 *M*)–NaCl (0.10 *M*). An additional series of experiments was run in HCl–NaCl solution at 2 *M* ionic strength at these pH values: −0.30 (2 *M* HCl), 0.00, 0.20, 1.0, 2.0, 3.0, and 4.6 (acetate buffer). Appropriate solutions were prepared according to Calvert and Pitts[10] for liquid phase, tris(oxalato)ferrate(III) chemical actinometry. Potassium tris(oxalato)ferrate(III) was prepared from reagent grade potassium oxalate and ferric chloride and recrystallized several times. The 1,10-phenanthroline (Aldrich) was used without purification.

Apparatus. Quantum yields were determined using a continuous beam photolysis apparatus consisting of a 200-W high-pressure mercury short-arc lamp (PEK Model 911 lamp housing) powered by a PEK Model 701-A power supply, a Jarrell-Ash Model 82-410 0.25-m monochromator, a quartz collimating lens, and a thermostated cylindrical cell holder, mounted in the sequence listed on a 1.25-m optical bench. The calculated band pass of the monochromator (equipped with 2-mm slits) is 6 nm. Three of the more intense lines of the mercury lamp (366, 405, and 436 nm) are in the charge-transfer region of the ruthenium(II) complexes studied, and photolyses were carried out at these wavelengths. Usable intensities generated by this apparatus averaged 0.7×10^{-7}, 0.9×10^{-7}, and 1.2×10^{-7} einstein min^{-1} cm^{-2} for wavelengths 405, 436, and 366 nm, respectively.

Most product studies were carried out using a similar optical train but with filters replacing the monochromator. The filter system, a modification of one reported by Calvert and Pitts,[11] consisted of a 5-cm quartz cell filled with aqueous tetraamminecopper(II) chloride (0.035 *M*) solution, a 5-cm cell filled with a carbon tetrachloride solution of iodine (0.06 *M*), and a Corning uv absorbing glass filter (0-51). This combination gave a transmission maximum at about 405 nm with a band pass of about 40 nm and a usable intensity of about 1.0×10^{-5} einstein min^{-1} cm^{-2}. A similar apparatus was used for the deuterium exchange experiments. The filter combination was an Oriel Optics Corp. interference filter (404.7 nm) plus an Oriel ir absorbing filter. The usable intensity of the photolysis beam averaged 5×10^{-6} einstein min^{-1} cm^{-2} with a band pass of 10 nm.

All spectra and optical density measurements were taken on a Cary 14 spectrophotometer. A Sargent-Welch Model NX digital pH meter calibrated against commercial buffers was employed for pH measurements. An Isco Model 270 fraction collector was used with the ion-exchange chromatography experiments.

Spectroscopic Quantum Yield Measurements. Light intensities were determined by ferrioxalate actinometry before each photolysis run. During most runs, the 2-cm pathlength quartz sample solution cell was thermostated at 25°. The sample solution was not stirred continuously but was agitated periodically during the photolysis experiment to ensure solution homogeneity. Solution samples were prepared for quantum yield runs under an argon atmosphere, in the dark, and in an all glass apparatus described previously for preparation of samples for rate studies.[12]

Quantum yields were measured spectroscopically as follows. Prior to photolysis, the spectrum of the sample solution was recorded to obtain accurate optical densities for the charge transfer λ_{max} (407 nm for L = pyridine) and for the wavelength of irradiation, λ_{irr} (405 nm for most runs with L = pyridine). The initial concentration of $Ru(NH_3)_5L^{2+}$ was calculated from the MLCT λ_{max} optical density. For most runs, the initial optical density at λ_{irr} fell in the range 1.0 ± 0.2; however, a number of runs were made at twice this concentration. After equilibration to the cell holder temperature, photolysis was begun by irradiating the sample for a period, usually 5.00 or 10.00 min. Following this, the sample was transferred to the spectrophotometer for measurements of absorbances at the MLCT λ_{max} and at λ_{irr}. All transfers were carried out using procedures to ensure minimal exposure to room light. This photolysis–analysis procedure was repeated four to ten times at which point the optical density at λ_{max} had decreased 30–50%, and the run was terminated. For control reactions, identical samples were submitted to this procedure but were not irradiated. Under the experimental conditions, dark reactions were insignificant for L = benzonitrile and L = 3-chloropyridine at all pH's and were significant for L = pyridine and L = 4-methylpyridine only at the lower pH's investigated.

The formula used to calculate the quantum yields, Φ_t, for the progressing reaction is

$$\Phi_t = (\Delta A V / l\epsilon)/(I_o^i t F)$$

where ΔA = the change in optical density at the MLCT λ_{max} from time 0 to time t (corrected for dark reaction); V = the volume of the photolysis cell (liters); l = the pathlength of the photolysis cell (cm); ϵ = the molar extinction coefficient of the complex (M^{-1} cm^{-1}); I_o^i = the output of the lamp (einsteins/min); t = irradiation time (min); and F = fraction of incident light absorbed (calculated from the average absorbances at λ_{irr}, 1 − antilog $[-(A_{irr_0} + A_{irr_t})/2]$, where A_{irr_0} is the absorbance at time zero and A_{irr_t} is the absorbance at time t). The use of average absorbances can only be valid if F is near 1; the experiments reported here fulfill this requirement. The method of evaluating F was checked several times by using actinometry to evaluate the fraction of light passing through the photolysis solution. In addition the extrapolated Φ_L values (see below) obtained in these photolysis experiments were independent of the initial concentration of complex giving values within the precision limits whether A_{irr_0} was about 1 or greater than 2.

The Φ_t values were plotted *vs.* t (or *vs.* per cent reaction), and the plot was extrapolated to $t = 0$. These plots proved linear, with a negative slope, for the first 25–30% of the reaction. The extrapolated spectroscopic quantum yield at $t = 0$ was taken as Φ_L, the quantum yield for the photoaquation of L from $Ru(NH_3)_5L^{2+}$ (see Results). Evaluation of Φ_L at $t = 0$ eliminates possible complications resulting from secondary photolysis of primary reaction products.[4b] Calculations of Φ_t and the least-squares extrapolations

London, 1970; (b) A. W. Adamson, W. L. Waltz, E. Zinato, D. W. Watts, P. D. Fleischauer, and R. D. Lindholm, *Chem. Rev.*, 68, 541 (1968).

(5) D. Valentine, Jr., *Advan. Photochem.*, 6, 123 (1968).

(6) (a) T. Kelly and J. F. Endicott, *J. Amer. Chem. Soc.*, 92, 5733 (1970); (b) L. Moggi, *Gazz. Chim. Ital.*, 97, 1089 (1967), as reported in ref 4b.

(7) W. L. Wells and J. F. Endicott, *J. Phys. Chem.*, 75, 3075 (1971).

(8) P. Ford, D. Rudd, R. Gaunder, and H. Taube, *J. Amer. Chem. Soc.*, 90, 1187 (1968).

(9) R. E. Clarke and P. C. Ford, *Inorg. Chem.*, 9, 227 (1970).

(10) J. G. Calvert and J. N. Pitts, "Photochemistry," Wiley, New York, N. Y., 1966, pp 783–786.

(11) Reference 10, p 736.

(12) P. C. Ford, J. R. Kuempel, and H. Taube, *Inorg. Chem.*, 7, 1976 (1968).

Table I. Spectra Maxima and Extinction Coefficients for Species Relevant to Photolyses and Product Studies

Complex ion	λ_{max}, nm ($\epsilon \times 10^{-3}$)[a] Charge transfer bands	Other bands	Ref
	Ru(II) Complexes		
$Ru(NH_3)_5py^{2+}$	407 (7.78)	244 (4.56)	*b*
$Ru(NH_3)_5(3\text{-}Cl\text{-}py)^{2+}$	426 (7.9)	256 (5.3)	*c*
$Ru(NH_3)_5(4\text{-}CH_3\text{-}py)^{2+}$	397 (7.7)	244 (4.6)	*c*
$Ru(NH_3)_5(C_6H_5CN)^{2+}$	376 (8.5), 347 sh (6.9)	249 (16.2), 226 (14.8)	*d*
cis-$Ru(NH_3)_4(H_2O)py^{2+}$	400 (6.6)	244 (4.5)	*c*
trans-$Ru(NH_3)_4(H_2O)py^{2+}$	403 (7.8)	243 (5.6)	*c*
cis-$Ru(NH_3)_4(py)_2^{2+}$	408 (10.5), 375 sh (9.6)		*e*
trans-$Ru(NH_3)_4(py)_2^{2+}$	423 (15.7)		*e*
	Ru(III) Complexes		
$Ru(NH_3)_5Cl^{2+}$	328 (1.93)		*f*
cis-$Ru(NH_3)_4Cl_2^{+}$	350 (1.48), 308 (1.28)	263 sh (0.46)	*c*
trans-$Ru(NH_3)_4Cl_2^{+}$	331 (4.95), 295 sh (0.71)		*c*
$Ru(NH_3)_5py^{3+}$		253 (4.53)	*b*
cis-$Ru(NH_3)_4Cl(py)^{2+}$	342 (1.94)	263 (3.9)	*c*
trans-$Ru(NH_3)_4Cl(py)^{2+}$	343 (2.76)	253 (4.5)	*c*
pyH^{+}		255 (5.25)	*b*

[a] Units M^{-1} cm^{-1}. [b] Reference 8. [c] This work. [d] Reference 9. [e] The extinction coefficients for *cis*- and *trans*-$Ru(NH_3)_4(py)_2^{2+}$ represent modest corrections of those reported in ref 14. [f] Reference 16.

were carried out using programs written for a Hewlett-Packard Model HP 9100A table-model computer. The Φ_L values were determined from three to ten times for each set of conditions reported in the Results with an average precision of ±4%. Similar agreement was obtained between Φ_L values obtained independently at particular sets of conditions by different individuals in this laboratory, although both precision and agreement between independently obtained sets of data were less good under conditions where dark reaction corrections were significant.

Deuteration Experiments. The possibility of exchange between solution H^+ and the pyridine ring hydrogens during MLCT excitation was examined. Typically a deaerated D_2O solution of D_2SO_4 (0.1 *M*) and $[Ru(NH_3)_5py][BF_4]_2$ (~0.02 *M*) was irradiated in a 5-cm cylindrical quartz cell (15-ml volume). During photolysis, the solution was stirred continually by an externally mounted magnetic stirrer. Irradiation time ranged from 15 to 20 hr, so that the number of einsteins incident on the cell equalled 15 ± 1 times the moles of complex initially present. After irradiation, the photolysis solution was quenched by oxidation with atmospheric oxygen, and then solid NaOH (sufficient to give a strongly alkaline solution) was added to neutralize the free pyridinium ion and to displace coordinated pyridine. Solid NaCl was then added until the brown solution was saturated. This mixture was placed in a liquid–liquid continuous extractor and extracted with diethyl ether for a period of 12–24 hr. The resulting ether extract (containing most of the original pyridine) was concentrated by distillative removal of the ether and then submitted to vapor-phase chromatography, and the pyridine fraction was collected. Mass spectra of this sample were obtained using a Finnegan Model 1015 mass spectrometer equipped with a Moseley 7101B strip chart recorder. Per cent deuteration of the pyridine was calculated from the intensities of masses 79 (parent, C_5H_5N), 80 (parent +1), and 81 (parent +2) after taking account of natural abundances displayed by a reagent pyridine spectrum taken the same day.

For a control experiment pyridine (0.02 *M*) was irradiated under identical conditions in 0.1 *M* D_2SO_4–D_2O solution, and a similar solution of $[Ru(NH_3)_5py][BF_4]_2$ (2.2×10^{-2} *M*) was subjected to conditions analogous to the photolysis experiments with no irradiation. Identical methods were used to recover and to analyze the pyridine from these experiments.

Product Studies. Photolysis product study solutions were prepared in the dark under an inert atmosphere. A 50-ml portion of the buffer solution was used to dissolve the solid sample (10–25 mg) in a mixing flask from which aliquots could be withdrawn by syringe and transferred to deaerated spectroscopic cells. The optical densities of these aliquots were used to calculate solution concentrations. The photolysis solution was then transferred to a 10-cm quartz photolysis cell with two necks, one fitted with a stopcock and the other with a serum cap. During photolysis, the solution was stirred by a small magnetic bar in the cell. The reaction was run to 30–40% completion after which a measured volume of the sample was withdrawn by syringe, acidified with 3 *M* HCl (2 ml), and then slowly oxidized with O_2. As the Ru(II) is oxidized to the substitution inert Ru(III), chloride ions substitute into coordination sites previously occupied by H_2O. The resulting solution of Ru(III) complexes is sufficiently stable to be analyzed by cation exchange on Dowex AG 50W-X4 resin.[12] Thermal (dark) control reactions were carried out and analyzed in an analogous manner.

The quantum yields for the photoaquation of the ammonias cis and trans to the pyridine were obtained by analysis of the ruthenium photoproducts, since published methods[12,13] for quantitatively measuring elution aliquot NH_4^+ concentration proved too irreproducible. However, *cis*- and *trans*-$[Ru(NH_3)_4pyCl]^{2+}$ elute together, and their relative concentrations cannot be determined by the spectroscopic analysis of the elution aliquots. A technique of "double elution" was developed to separate the cis and trans isomers. After elution in the normal manner, the combined aliquots containing *cis*- and *trans*-$[Ru(NH_3)_4pyCl^{2+}]$ were deaerated with argon and then reduced over zinc amalgam. Deaerated pyridine (0.5 ml) was added to this solution to give the corresponding *cis*- and *trans*-bis(pyridine) complexes $Ru(NH_3)_4(py)_2^{2+}$, reactions which occur with stereochemical retention of configuration.[14] After several hours, the ruthenium solution was filtered, acidified, and then oxidized with hydrogen peroxide. The *cis*- and *trans*-$Ru(NH_3)_4(py)_2^{3+}$ isomers were separated by ion exchange, the cis isomer eluting first, and were analyzed spectrophotometrically.

Extinction Coefficients. The extinction coefficients of *cis*- and *trans*-$Ru(NH_3)_4py(H_2O)^{2+}$ and *cis*- and *trans*-$Ru(NH_3)_4pyCl^{2+}$ were measured by the procedure described for the cis isomers. In the dark, a deaerated solution of *cis*-$Ru(NH_3)_4Cl_2^{+}$ (0.005 g) and pyridine (0.0015 g) was reduced over zinc amalgam for 30 min. The solution was then filtered and acidified with HCl, and the Ru(II) species were oxidized to Ru(III) by O_2. Ion exchange cleanly separated *cis*-$Ru(NH_3)_4pyCl^{2+}$ from the other species present, *cis*-$Ru(NH_3)_4Cl_2^{+}$ and *cis*-$Ru(NH_3)_4(py)_2^{3+}$. A portion of the aliquot containing *cis*-$Ru(NH_3)_4pyCl^{2+}$ was deaerated in a spectrophotometer cell and the spectrum recorded. The solution was then reduced with a measured volume of Cr^{2+} solution to give *cis*-$Ru(NH_3)_4py(H_2O)^{2+}$. The spectrum was recorded and then deaerated pyridine was added to generate *cis*-$Ru(NH_3)_4(py)_2^{2+}$. After formation of the latter species was complete, the spectrum was recorded and the concentration of Ru(II) in the sample was calculated using the extinction coefficients of *cis*-$Ru(NH_3)_4(py)_2^{2+}$ (dilutions and spectra of control solutions were taken into consideration). The extinction coefficients of *cis*-$Ru(NH_3)_4py(H_2O)^{2+}$ and *cis*-$Ru(NH_3)_4pyCl^{2+}$ were then calculated from the concentrations of ruthenium and the optical densities from relevant spectra.

The extinction coefficients of *cis*- and *trans*-$Ru(NH_3)_4(py)_2^{2+}$ were redetermined by reducing *cis*- or *trans*-$Ru(NH_3)_4Cl_2^{+}$ with Cr^{2+} in the presence of pyridine to generate the *cis*- or *trans*-$Ru(NH_3)_4(py)_2^{2+}$. The optical densities at the MLCT λ_{max} were measured to give the extinction coefficients. Quantitative spectra of the $Ru(NH_3)_5(4\text{-}CH_3\text{-}py)^{2+}$ and $Ru(NH_3)_5(3\text{-}Cl\text{-}py)^{2+}$ tetrafluoroborate salts

(13) W. T. Bolleter, C. J. Bushman, and P. W. Tidwell, *Anal. Chem.*, **33**, 592 (1961).

(14) P. C. Ford and C. Sutton, *Inorg. Chem.*, **8**, 1544 (1969).

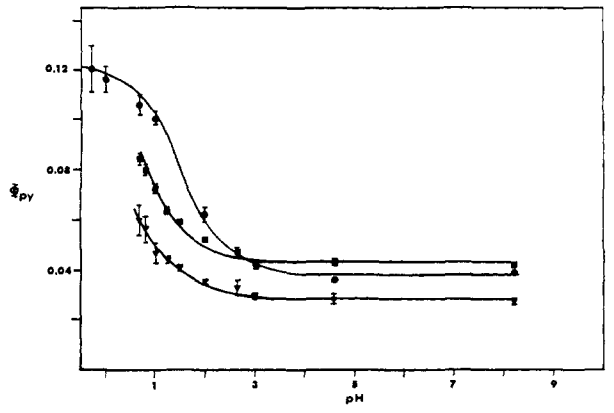

Figure 1. Plot of Φ_{py} *vs.* pH for the 405-nm photolyses of $Ru(NH_3)_5py^{2+}$ in aqueous chloride solution (25°, initial complex concentration *ca.* 1×10^{-4} *M*). Circles: Φ_{py}(spectroscopic) for $\mu = 2.0$ *M*; solid line represents theoretical curve based on eq 8. Squares: Φ_{py}(spectroscopic) for $\mu = 0.20$ *M*; solid line represents theoretical curve based on eq 8. Triangles: Φ_{py}(eluted), $\mu = 0.20$ *M*; solid line for illustrative purposes only. Data corrected for dark reactions.

were obtained for solutions prepared gravimetrically under an inert atmosphere. The extinction coefficients pertinent to the results reported here are presented in Table I. Because of the complicated procedures used to obtain certain spectra, extinction coefficient experimental uncertainties are about ±10% for *cis*- and *trans*-$Ru(NH_3)_4(H_2O)py^{2+}$ and *cis*- and *trans*-$Ru(NH_3)_4Cl(py)^{2+}$.

Results

All quantum yields reported are for the photolyses of visible-range MLCT bands of the complexes $Ru(NH_3)_5L^{2+}$, where L is pyridine, 3- chloropyridine, 4-methylpyridine, or benzonitrile. The spectra of these and similar species have been discussed previously.[8,9,15] In a preliminary communication[1a] we reported that photolysis of these MLCT bands leads only to photoaquation. This conclusion is based on three observations. (1) Addition of excess pyridine to $[Ru(NH_3)_5py][BF_4]_2$ solution, after 50% MLCT photolysis induced decrease in the 407-nm absorbance, leads to nearly complete regeneration of this band's intensity. (2) MLCT photolysis in chloride solution does not lead to detectable formation of $Ru(NH_3)_5Cl^{2+}$ [λ_{max} 328 nm (ϵ 1930)][16] prior to oxidative quenching. The absorption band for this species occurs at an optical density minimum of the $Ru(NH_3)_5py^{2+}$ and is easily detected in the spectrum of the MLCT-photolyzed solution after traces of oxygen have been introduced. Although $Ru(NH_3)_5py^{3+}$ might be expected to be the primary photooxidation product, the Ru(III)/Ru(II) redox potential is significantly greater for pentaamminepyridine coordination (0.42 V)[17] than for aquopentaammine coordination (0.16 V).[18] Consequently, a mixture of the expected photooxidation product $Ru(NH_3)_5py^{3+}$ and the photoaquation product $Ru(NH_3)_5H_2O^{2+}$ would give $Ru(NH_3)_5H_2O^{3+}$ (eq 1)

$$Ru(NH_3)_5py^{3+} + Ru(NH_3)_5H_2O^{2+} = Ru(NH_3)_5py^{2+} + Ru(NH_3)_5H_2O^{3+} \quad (1)$$

which in the presence of chloride and catalytic $Ru(NH_3)_5H_2O^{2+}$ would form $Ru(NH_3)_5Cl^{2+}$ (eq 2) as

$$Ru(NH_3)_5H_2O^{3+} + Cl^- \underset{\text{catalytic } Ru(NH_3)_5H_2O^{2+}}{\rightleftharpoons} Ru(NH_3)_5Cl^{2+} + H_2O \quad (2)$$

the more stable Ru(III) species.[19] Since Ru(II)/Ru(III) redox reactions are rapid,[18] $Ru(NH_3)_5Cl^{2+}$ should be the photooxidation product; yet none is observed when $Ru(NH_3)_5py^{2+}$ solutions are photolyzed at 405 nm under rigorously deoxygenated conditions. (3) The yields of photoaquation products (see below) determined by ion-exchange elution confirm that the spectroscopic quantum yields reflect photoaquation pathways.

Spectroscopic Quantum Yields for $Ru(NH_3)_5py^{2+}$. The spectroscopic method for measuring quantum yields is outlined in the Experimental Section. The Φ determined is for the disappearance of the MLCT absorption. That this value represents the quantum yield for pyridine photoaquation (eq 3a) is dependent on the following ob-

$$H_2O + Ru(NH_3)_5py^{2+} \xrightarrow{h\nu} \begin{cases} \longrightarrow Ru(NH_3)_5H_2O^{2+} + py & (3a) \\ \longrightarrow cis\text{-}Ru(NH_3)_4(H_2O)py^{2+} + NH_3 & (3b) \\ \longrightarrow trans\text{-}Ru(NH_3)_4(H_2O)py^{2+} + NH_3 & (3c) \end{cases}$$

servations. First, photooxidation is at most a minor pathway and in addition would not lead to a decrease in $[Ru(NH_3)_5py^{2+}]$ owing to the reduction of the $Ru(NH_3)_5py^{3+}$ by aquo- or chloroammineruthenium(II) photoaquation products (eq 1). Second, pyridine, pyridinium ion, and the aquoammineruthenium(II) products of pyridine photoaquation are essentially transparent for the concentrations and wavelength region (407 nm) used for analysis. Third, the other primary photoaquation pathways, eq 3b and 3c, lead to only modest optical density decreases of the charge-transfer band owing to the spectral similarities of the ammonia aquation products *cis*-$Ru(NH_3)_4(H_2O)py^{2+}$ and *trans*-$Ru(NH_3)_4(H_2O)py^{2+}$ to the starting material (Table I). The extinction coefficients at 407 nm of $Ru(NH_3)_5py^{2+}$, *trans*-$Ru(NH_3)_4(H_2O)py^{2+}$, and *cis*-$Ru(NH_3)_4H_2Opy^{2+}$ are 7.78×10^3, 7.7×10^3, and 6.4×10^3 M^{-1}, respectively. Based on these values and on the ratios of pathways 3a, 3b, and 3c determined by the product studies, it appears that the spectroscopic quantum yield at most exceeds by 6–15% the actual pathway 3a quantum yield owing to the contributions from pathway 3b and depending upon reaction conditions. There is, however, no contribution (positive or negative) to the spectroscopic quantum yield from secondary photolysis of the aquotetraammine-pyridine products since the Φ_{py} values were determined by extrapolation to the $t = 0$ intercept.

The spectroscopic quantum yields Φ_{py} for $Ru(NH_3)_5py^{2+}$ MLCT photolysis are reported in Figure 1. For each set of conditions where the pH is greater than 3.0, the Φ_{py} values are uncomplicated by dark reactions. Furthermore, there appears to be no dependence on the irradiation intensity over the range employed for these studies [$I = (0.4\text{–}1.5) \times 10^{-5}$ einstein/(l. min)]. However, for pH's less than 2.0, dark reaction corrections are necessary for the Φ_{py} values. At no pH was a Φ_{py} dependence on $Ru(NH_3)_5py^{2+}$ concentration noted over the range 3.7×10^{-5} *M*–18.3×10^{-5} *M*.

(15) A. M. Zwickel and C. Creutz, *Inorg. Chem.*, **10**, 2395 (1971).
(16) H. Hartman and C. Buschbeck, *Z. Phys. Chem. (Frankfurt am Main)*, **11**, 120 (1957).
(17) R. G. Gaunder and H. Taube, *Inorg. Chem.*, **9**, 2627 (1970).
(18) T. J. Meyer and H. Taube, *ibid.*, 7, 2369 (1968).
(19) J. F. Endicott and H. Taube, *ibid.*, 4, 437 (1965).

However, at the lower pH's significant differences were observed between Φ_{py} values measured at 0.2 *M* ionic strength (NaCl–HCl) and at 2.0 *M* ionic strength (NaCl–HCl). Plots of spectroscopic quantum yields *vs.* pH (Figure 1) display reverse "S" curves plateauing at ~0.04 mol/einstein for both chloride concentrations at pH's greater than 3.0. At lower pH's, the Φ_{py} values appear to show a saturation in their dependence on $[H^+]$ leveling at ~0.12 einstein/mol for μ = 2.0 *M* chloride. For the Φ_{py} values determined at 0.20 *M* chloride concentration, a similar saturation is indicated but not definitively shown at the low pH limit (0.20 *M* HCl). In a previous communication[1b] from this laboratory, Φ_{py} values determined at 0.20 *M* chloride concentrations were reported, and these values more definitively indicated saturation effects at the lowest pH's. These data were somewhat in error at the lower pH's owing to overcompensation for the acid-catalyzed thermal aquation[12] of $Ru(NH_3)_5py^{2+}$. The 0.2 *M* chloride solution data reported here represent a new and entirely independent series of quantum yield determinations for which thermal control reactions were carried out on samples of the same solutions as those samples photolyzed. The importance of the thermal reaction leads to the larger experimental uncertainties observed at the lower pH's.

Spectroscopic quantum yields Φ_L were also determined over a wide pH range for the $Ru(NH_3)_5^{2+}$ complexes of 3-chloropyridine, 4-methylpyridine, and benzonitrile (Figure 2). The 4-methylpyridine complex displayed a pH profile for the Φ_L values similar to that observed for the pyridine complex (Figure 2), while over the same pH range (0.7–9.0) the 3-chloropyridine and benzonitrile complexes displayed no sensitivity to pH. However, the Φ_L value for the 3-chloropyridine complex in 2.0 *M* aqueous HCl solution is about 30% higher than Φ_L for the comparable experiment run at pH 3.0 in 2 *M* NaCl solution. Within the experimental uncertainty of the data obtained (~10%), the quantum yield for L = benzonitrile is not affected by acid.

Product Studies. The cation-exchange method of determining product distributions requires significantly more material than the spectroscopic quantum yield determinations. Consequently, studies to quantify the ruthenium products were carried out both at higher complex concentrations ($\sim 8 \times 10^{-4}$ *M*) and at higher irradiation intensities [3×10^{-4} einstein/(l. min)] than were the spectroscopic studies. After irradiation, the ruthenium solutions were oxidized and then ion exchanged as the Ru(III) complexes. Species[20] eluted included *cis*- and *trans*-$Ru(NH_3)_4Cl_2^+$ (traces), pyridinium ion, ammonium ion, $Ru(NH_3)_5Cl^{2+}$, *cis*- and *trans*-$Ru(NH_3)_4pyCl^{2+}$, and $Ru(NH_3)_5py^{3+}$. The concentrations of pyridinium ion and of $Ru(NH_3)_5py^{3+}$ were determined accurately from the spectra of the elution aliquots. From these were calculated the extents of pyridine photoaquation (after correction for dark reaction) and of total photoreaction, respectively. The species recovered can be summed in two ways to determine whether a respectable mass balance exists between the amounts of $Ru(NH_3)_5py^{2+}$ in the original photolysis solutions and of the species isolated (Table II). The

(20) For the NH_3/NH_4^+ buffer solution, no attempt was made to quantify the Ru^{III} chloro complex concentration owing to the reaction of the Ru(II) aquo complexes with NH_3 to form the substitution inert (relatively) ammine complexes according to the equations: $Ru(NH_3)_5H_2O^{2+} + NH_3 \rightarrow Ru(NH_3)_6^{2+}$; $Ru(NH_3)_4(H_2O)py^{2+} + NH_3 \rightarrow Ru(NH_3)_5py^{2+}$. These reactions, while not complete, severely decreased the amounts of Ru(III) chloro species eluted in the ion-exchange analyses.

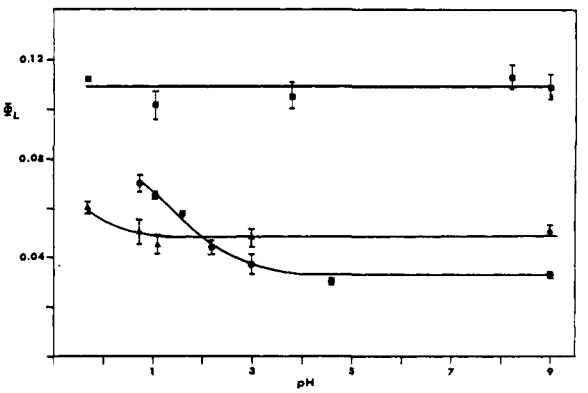

Figure 2. Φ_L *vs.* pH for the photolyses of various $Ru(NH_3)_5L^{2+}$ complexes: squares, L = benzonitrile; circles, L = 4-methylpyridine; triangles, L = 3-chloropyridine. Solid line curves are for illustrative purposes only. Data corrected for dark reactions. General conditions: 25°, μ = 0.20 except at pH −0.3, average concentration of complex $\sim 0.4 \times 10^{-4}$ *M*; 4-methylpyridine complex irradiated at 405 nm, 3-chloropyridine complex at 436 nm, and benzonitrile complex at 366 nm.

Table II. Amounts (mol) of Products Isolated by Cation-Exchange Chromatography of a Quenched $Ru(NH_3)_5py^{2+}$ Photolysis Solution[a]

Species eluted	Mol[b] × 10^6
pyH^+	4.3
$Ru(NH_3)_5Cl^{2+}$	2.7
cis-$Ru(NH_3)_4Cl(py)^{2+}$	2.6[c]
trans-$Ru(NH_3)_4Cl(py)^{2+}$	0.6[c]
$Ru(NH_3)_5py^{3+}$ (eluted)	9.2
Σ pyridine species eluted	16.7
Σ ruthenium species eluted	15.1
$Ru(NH_3)_5py^{2+}$ (initial)	16.3

[a] T = 24 ± 1°, pH 0.72. [b] Uncorrected for dark reactions. [c] By double elution procedure.

pyridine species, pyridinium ion and the pyridine complexes, have distinctive spectra and are the more stable toward secondary thermal reactions[12] among the products. The sum of these is usually somewhat high (~5%), the small discrepancy apparently due to the procedure for determining the initial concentration (Experimental Section). Ruthenium species eluted may also be summed; however, this result is usually lower than the sum of the pyridine species owing to the thermal instability of the aquoammineruthenium(II) products of pyridine aquation.[12] These aquoammine species are especially unstable at lower pH's where the discrepancy between the amounts of pyridinium ion and $Ru(NH_3)_5Cl^{2+}$ isolated is the largest.

The results of the product study experiments were (within generous error limits) internally consistent; however, the pyridine aquation quantum yields measured for these experiments were approximately 70% higher for the product studies than for the spectroscopic measurements. These differences most probably represent systematic errors in the light intensity measurements rather than any intrinsic reactivity differences between the two sets of experiments. For the product studies, the beam configuration (*e.g.*, band width and

Table III. Relative Quantum Yields for Ion-Exchange Product Studies[a]

pH	Φ_{py}	Φ_{cis}	Φ_{trans}	Φ_{NH_3}	Φ_{cis}/Φ_{trans}
0.72	2.21 ± 0.14	1.11 ± 0.21	0.31 ± 0.04	1.42 ± 0.25	3.6 ± 1.1
1.5	1.17 ± 0.18				
4.6	1.00 ± 0.097	1.15 ± 0.06	0.41 ± 0.07	1.56 ± 0.13	2.8 ± 0.7
8.2	1.01	1.10	0.27	1.37	4.1
9.5	1.22 ± 0.14				

[a] $T = 25°$; $\lambda_{irr} = 405$ nm; $I_0 = 3 \times 10^{-4}$ einstein/(l. min); all reactions corrected for thermal reactions; $[Ru(NH_3)_5py^{2+}]_{initial} = \sim 8 \times 10^{-4}$ *M*.

shape when focused) and intensity and cell configuration are significantly different than for the corresponding spectroscopic measurements. The internal consistency of the product study quantum yields suggests that the relative values are valid, and, for this reason, the relative rather than the absolute quantum yields are reported in Table III. Several features from the product studies stand out. (1) Despite the absolute value difference, the pyridine photoaquation quantum yield displays a dramatic increase at low pH similar to that illustrated in Figure 2 for the spectroscopic quantum yield. (2) The quantum yield (Φ_{NH_3}) for ammonia aquation is apparently invariant with pH. (3) The ratio Φ_{cis}/Φ_{trans} (while subject to substantial experimental uncertainty) is approximately 3.5 which is near the statistical ratio of 4. This result indicates that there is no dramatic bias favoring either cis or trans ammonia photoaquation products.

Since differences were observed between the spectroscopic quantum yields and the direct product study quantum yields measured at higher complex concentrations and beam intensities, cation-exchange product studies were carried out on samples for which spectroscopic quantum yields could also be measured. Lower concentrations ($\sim 10^{-4}$ *M*) and the lower intensity, monochromator selected wavelength irradiation [405 nm, 0.6×10^{-5} einstein/(l. min)] were the case, and the beam and cell configurations were identical with other spectroscopic experiments. At these concentrations, the pyridinium ion is the only product quantitatively measurable in the ion-exchange eluent samples. After determining the spectroscopic quantum yield, Φ_{py}(spectroscopic), in the normal manner, the photolysis solution was quenched and eluted from the cation-exchange column. The quantum yield of eluted pyridinium ion, Φ_{py}(eluted), is only about 65–70% of Φ_{py}(spectroscopic) measured on the same solution (Figure 1). However, this is the expected result because (1) the product study work-up inevitably leads to some material loss, (2) Φ_{py}(spectroscopic) overestimates pyridine photoaquation owing to the not quite ideal spectral match between starting material and the primary products of ammonia photoaquation, and, most importantly, (3) Φ_{py}(spectroscopic) is extrapolated to a time 0 (higher) value to eliminate contributions from secondary photolysis. Nonetheless, the value of Φ_{py}(eluted) displays a sensitivity to solution pH comparable to that observed for Φ_{py}(spectroscopic) (Figure 1).

Deuteration Experiments. Several photolyses were carried out in acidic D_2O solution to determine whether the MLCT excited state of $Ru(NH_3)_5py^{2+}$ is susceptible to protonation on a pyridine ring carbon position. This possibility which should lead to H/D exchange on the pyridine is suggested by the enhancement of pyridine electron density expected for the charge-transfer excited state.[8] Solutions of $[Ru(NH_3)_5py][BF_4]_2$ in acidic D_2O (0.1 *M* D_2SO_4) were irradiated with 405-nm light; pyridinium ion produced by photoaquation and coordinated pyridine were isolated and analyzed as one component. Mass spectra showed species with masses 80 (P + 1) and 81 (P + 2) having intensities measurably greater than the natural abundances. Quantum yields Φ_D calculated for total deuteration [(P + 1) + 2(P + 2) after corrections for natural abundances] were approximately 0.001 mol/einstein with deuteration of about 2% of the isolated pyridine. No deuteration was detectable when free pyridine was irradiated under identical conditions or when an identical D_2O–D_2SO_4 solution of $[Ru(NH_3)_5py][BF_4]_2$ was allowed to react in the dark.

Wavelength Dependence. $Ru(NH_3)_5py^{2+}$ was photolyzed at several wavelengths encompassed by the charge-transfer band. The conditions chosen were identical with those reported in Figure 1 for quantum yield measurements at pH 4.6. The wavelengths selected were the mercury lines at 366, 405, and 436 nm. The 405-nm line is very close to the MLCT maximum, and the 436- and 366-nm lines fall relatively far down the flanks of this band.[8] The quantum yields were 366 (0.043 ± 0.001), 405 (0.043 ± 0.001), and 436 nm (0.048 ± 0.001 mol/einstein). Though the differences are not large, it is interesting that the largest Φ_{py} (by 10–15%) is observed for the lowest energy irradiation wavelength.

Discussion

A metal-to-ligand charge-transfer transition can be conceptualized as leading to an excited state (CT*) having an oxidizing metal ion and a radical ion ligand in a coordination complex, *e.g.*

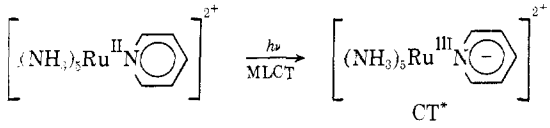

The chemical reaction properties of such a species are not obvious. The allowed transition from the $^1A_1$ ground state should give a singlet charge-transfer state which may undergo reaction itself, radiationless deactivation to $^1A_1$, internal conversion to ligand field excited state(s), or intersystem crossover to triplet excited states. Two potential consequences suggested by the formulation CT* are photooxidation of the ruthenium(II) and enhanced reactivity of the ligand electrophilic reactions. Oxidation of ruthenium has been reported[1a,21] for the photolyses of several pentaammineruthenium(II) complexes, $Ru^{II}(NH_3)_5L$, using unfiltered high-pressure mercury light sources (which provide a

(21) C. Sigwart and J. Spence, *J. Amer. Chem. Soc.*, **91**, 3991 (1969).

wide selection of middle uv and visible range frequencies). The fate of the reducing equivalents generated is not well understood; however, H_2 is a product[1a] in the photolyses of $Ru(NH_3)_5py^{2+}$ and $Ru(NH_3)_5(CH_3CN)^{2+}$. Complexes having L = py, CH_3CN, or N_2 each display MLCT spectral bands, but similar absorptions are not observed when L = NH_3 or H_2O. Consequently, the similarity of the reaction pathways observed[1a,21] for all these $Ru(NH_3)_5L^{2+}$ complexes suggests that the MLCT excited states are not necessary to the observed photooxidation of the ruthenium(II). No photooxidation is observed as the result of monochromatic irradiation of the $Ru(NH_3)_5py^{2+}$ MLCT band in deaerated chloride solution.

Previously, it was calculated[8] on the basis of spectral data that the MLCT excited state of the pentaammine-pyrazineruthenium(II) ion is about five orders of magnitude more basic than is the ground state (eq 4). This

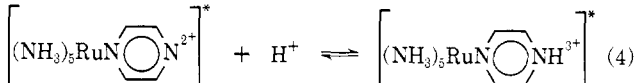

(4)

effect, consistent with the formulation CT* for the pyridine complex, suggests that the aromatic ring in the MLCT excited state may be more susceptible than the ground state to electrophilic reactions. In acidic D_2O solutions, electrophilic H/D exchange of pyridine protons indeed is observed as a photochemical pathway. However, the quantum yield Φ_D for deuteration is small ($\sim$0.001), suggesting that a carbon-protonated species is not a necessary intermediate in the acid-dependent pyridine photoaquation pathways (*vide infra*). Nonetheless, observation of photoinduced H/D exchange of the pyridine protons implies that at least one MLCT excited state has sufficient lifetime for bimolecular solution reactions. Recently, Zarnegar and Whitten[22] have reported that irradiation of MLCT absorption bands of bis(2,2′-bipyridine)bis(*trans*-4-stilbazole)ruthenium(II) leads to cis–trans isomerization of the 4-stilbazole ligand. Irradiation of ligand π–π^* bands gave different cis–trans isomer ratios indicating that, in their case, interconversion of the different excited states is slow compared with the ligand photoreactions. The observed isomerization is consistent with a CT*-like excited state having electron density in ligand antibonding orbitals.

Besides the low quantum yield H/D exchange, only photoaquations (eq 3) are observed as the result of irradiation of the $Ru(NH_3)_5py^{2+}$ MLCT absorption bands. It is unclear whether an MLCT excited state should be aquation labile. The electron promoted from the low-spin d^6 Ru(II) has π symmetry with respect to the metal–ligand bond axis, and the σ-metal–ammonia bonds and the σ component of the Ru–py bond should be unaffected or perhaps enhanced owing to the more positive nature of the ruthenium in the excited state. The π component of the Ru–py bond is, no doubt, less important in the excited state. However, since metal-to-ligand π backbonding is relatively insignificant to the stability of ruthenium(III) complexes,[8,9] it is improbable that a ligand in a charge-transfer state such as CT* would be noticeably more substitution labile than in the corresponding Ru(III) compound. Under the photolysis conditions, neither NH_3 nor pyridine of $Ru(NH_3)_5py^{3+}$ are substitution labile, suggesting that CT* may be substitution inert.

Photoaquation potentially could occur by radiationless deactivation of an excited state to produce a vibrationally "hot" ground-state complex which undergoes aquation. Such a species might lead to competitive pyridine and ammonia aquations (providing vibrational modes are not selectively excited in the deactivation process),[23] since similar competition occurs[12] in thermal aquations of $Ru(NH_3)_5py^{2+}$. Conceivably, quantum yields for photoaquation by this pathway may be dependent on the energy of absorbed light,[4b] a prediction contrary to our observations. However, it is also likely that thermal equilibration occurs in the electronic excited state prior to deactivation, thus washing out any potential wavelength dependence.[23] Vibrational relaxation in fluid, condensed media should be sufficiently rapid to rule out a vibrationally "hot" species from participation in the observed bimolecular acid-dependent photoaquation pathways. Nonetheless, the present data do not completely rule out this mechanism as a contributor to acid-independent photoaquation.

If a single electronic state is responsible for the competitive photoaquation of pyridine, *cis*-ammonia, and *trans*-ammonia, it is probable that this would be a ligand field excited state generated by interconversion from the manifold of charge-transfer states. For an octahedral Ru(II), this would have the electronic configuration $(t_{2g})^5(e_g)^1$ with an electron in a σ-antibonding d orbital. Such a state should prove significantly more labile than the ground state and perhaps display some preference toward pyridine aquation owing to decreased π bonding and to the weaker Lewis basicity of pyridine. We believe that ammonia photoaquation and probably at least part of the pyridine photoaquation most likely occur *via* ligand field excited state(s).

The pH Effect on the Pyridine Photoaquation Quantum Yields. The most surprising feature of the work reported here is the sensitivity of the pyridine photoaquation quantum yields, Φ_{py}, to medium effects, especially pH. In contrast, Φ_{NH_3} for aqueous $Ru(NH_3)_5py^{2+}$ appears to be pH independent. The pH sensitivity of Φ_{py} is not a result of protonation of the ground state, as the spectrum of the reaction solution prior to photolysis is independent of the acid concentration. In addition, the effect is not due to the suppression of a thermal back reaction[24] since the effect would be most dramatic at pH's near the pK_a of free pyridine (5.3) rather than at the much lower pH's observed. Consequently, the pH dependence of Φ_{py} must be the result of a specific interaction between H^+ and either an excited state or short-lived intermediate leading to pyridine aquation. The "S" curve for Φ_{py} *vs.* pH (Figure 1) requires competitive acid-dependent and acid-independent pyridine photoaquation pathways and a competitive, independent pathway from the excited state(s) or intermediate(s) to starting material. In addition, since Φ_{NH_3} is pH independent, the role of H^+ in pyridine photoaquation must occur *after* the ammonia aquation and the potentially acid-dependent pyridine aquation pathways have branched.

(22) P. P. Zarnegar and D. G. Whitten, *J. Amer. Chem. Soc.*, **93**, 3776 (1971).

(23) E. W. Schlag, S. Schneider, and S. F. Fischer, *Annu. Rev. Phys. Chem.*, **22**, 465 (1971).

(24) R. J. Allen and P. C. Ford, *Inorg. Chem.*, **11**, 679 (1972).

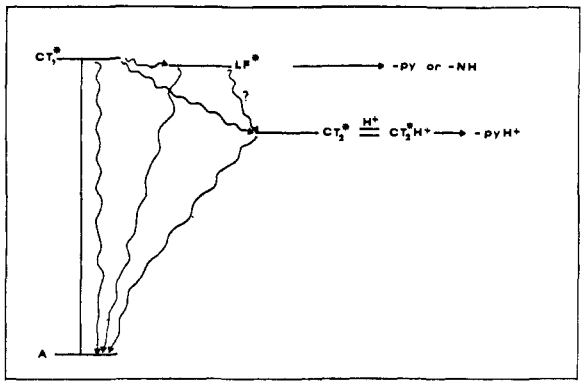

Figure 3. A possible scheme leading to acid-catalyzed photoaquation of pyridine from a charge-transfer excited state (mechanism II) (for —NH in figure, read $-NH_3$).

In a previous communication,[1b] we proposed a kinetic scheme (eq 5–8) which would account for the pH de-

$$[Ru(NH_3)_5(py)]^{2+} \underset{k_3}{\overset{h\nu,\ \Phi_A}{\rightleftharpoons}} \underset{A}{\{(NH_3)_5Ru^{II}\cdots py\}} \quad (5)$$

$$H_2O + A \xrightarrow{k_1} [Ru(NH_3)_5(H_2O)]^{2+} + py \quad (6)$$

$$H_3O^+ + A \xrightarrow{k_2} [Ru(NH_3)_5(H_2O)]^{2+} + pyH^+ \quad (7)$$

$$\Phi_{py} = \Phi_A\left(\frac{k_1 + k_2[H^+]}{k_1 + k_3 + k_2[H^+]}\right) \quad (8)$$

pendence of Φ_{py} where Φ_A is a quantum yield for the formation of A. For the values $\Phi_A = 0.122$ mol/einstein, $k_2 = (120\ M^{-1})k_1$, and $k_3 = 2.21\ k_1$, the curve generated by eq 8 adequately fits the Φ_{py} values determined at 2.00 M ionic strength, and for $\Phi_A = 0.122$ mol/einstein, $k_2 = (20\ M^{-1})k_1$, and $k_3 = 1.8k_1$, the curve generated fits Φ_{py} at $\mu = 0.2\ M$ (Figure 1).[25] The implicit assumption in this scheme (mechanism I) is that all pyridine aquation occurs *via* a common intermediate A for bimolecular reaction with H^+. Since an analogous species $(NH_3)_4$-$pyRu^{II}\cdots NH_3)^{2+}$ can be envisioned as an intermediate for the ammonia aquation pathways, absence of an acid dependence for Φ_{NH_3} could result from a lifetime insufficient for reaction with H^+. Pyridine, however, has a possible bonding mode not available to NH_3; the pyridine ring could turn 90° with respect to the normal Ru^{II}–N bond axis and enter into a π complex with the $Ru(NH_3)_5^{2+}$. The possibility of such a species draws support from rate studies[26] of the linkage isomerization of the ^{15}N-labeled dinitrogen complex $(NH_3)_5Ru^{15}NN^{2+}$ which imply that the intermediate perpendicular configuration a, although much less stable than the normal configuration b, has residual bonding.

$$Ru^{II}\text{–}\overset{N}{\underset{N}{\|}}$$

a

$$Ru^{II}\text{–}N\equiv N$$

b

A schematic of pathways (mechanism II) utilizing protonic interaction with an excited state to explain the pH effect on Φ_{py} is shown in Figure 3. In this mechanism, the acid-independent pyridine and ammonia aquation pathways are proposed to occur *via* a ligand field excited state(s) (LF*) and the acid-dependent pyridine aquation pathway *via* a second MLCT excited state (CT_2*, probably triplet). The branching of the acid-dependent and acid-independent paths would be satisfied by the requirement that the state LF* cannot be populated by internal conversion and/or intersystem crossover from CT_2* since NH_3 aquation is apparently pH independent. Energetically, this requirement is within reason, especially if LF* is a singlet. Low-intensity $^1T_{1g} \leftarrow {}^1A_1$ ligand field absorption bands of Ru(II) hexaamines[27] are comparable in energy to the MLCT absorption bands photolyzed in this study, so singlet ^{1}LF* states no doubt are populated by internal conversion from *CT. Little is known about the energies of triplet LF* states of Ru(II) ammines. However, one can estimate from luminescence data published[28] for the hexaammine and pentaammine complexes of rhodium(III) (also $4d^6$) that the lowest triplet ligand field excited state energy may be comparable or even lower than the lowest triplet charge-transfer state for these ruthenium(II) complexes. In mechanism II, the pH effect on Φ_{py} would result from protonation of the coordinated pyridine ring[29] of CT_2* followed by loss of pyridine from the coordination sphere. The feasibility of such a mechanism is demonstrated by the observation of the photolysis-induced pyridine H/D exchange in acidic D_2O. However, the quantum yield for H/D exchange is more than an order of magnitude too small for the acid-catalyzed photoaquation pathway to involve a fully developed carbon-protonated intermediate. On the other hand, a pathway where the catalytic proton and a proton originally on the aromatic ring do not become equivalent (*e.g.*, protonation of the CT* aromatic π electrons) is not excluded.

Recent flash photolysis[30] studies of the pyridine and benzonitrile complexes have shown transient bleaching of the MLCT bands followed by slow regeneration of starting material. The substrate is not completely regenerated, thus confirming the photochemistry[1] of these ions. The transient responsible for regeneration of substrate is long lived (on the order of milliseconds), and the rate law for regeneration is acid independent for the benzonitrile complex but contains a term inverse in acid concentration for the pyridine complex. These data are most easily reconciled with mechanism II, and it has been proposed[30] that protonation of the charge-transfer state occurs at the pyridine nitrogen (to give a tetrahedral coordinated nitrogen). However, these data can perhaps also be reconciled with a scheme similar to mechanism I where the intermediate A is reversibly protonated and is thus stabilized, rather than destabilized,[1b] relative to substrate or products.

Ionic Strength. In Figure 1, the general appearance of Φ_{py} ($\mu = 0.2\ M$) as a function of pH is similar to that

(25) A somewhat different set of values for k_2, k_3, and Φ_A were proposed in a previous communication[1b] to fit similar data obtained at 0.2 M ionic strength; however, in that case Φ_A was underestimated owing to overcompensation for dark reactions at low pH.

(26) J. N. Armor and Henry Taube, *J. Amer. Chem. Soc.*, 92, 2560 (1970).

(27) P. C. Ford, *Coord. Chem. Rev.*, 5, 75 (1970).

(28) T. R. Thomas and G. A. Crosby, *J. Mol. Spectrosc.*, 38, 118 (1971).

(29) We discount protonation of the metal as unlikely for a charge transfer or ligand field excited state, since in the former case electron density has been moved radially away from the metal, decreasing not increasing metal basicity, and in the latter case electron density has been transferred angularly away from the stereochemically available octahedral faces. Of the two types, the ligand field states would be expected to show the greater metal basicity.

(30) Private communication from J. Endicott.

of Φ_{py} (μ = 2.0 M) with two principal differences. At the lower ionic strength, the lowest pH possible was insufficient to attain a Φ_{py} plateau, and the acid-dependent pathway begins to take effect at a lower pH. The latter observation, a shift of the Φ_{py} *vs.* pH curve to the left, indicates a decreased sensitivity of the system to H^+ concentration. Regardless of the actual mechanism, the observation of decreased sensitivity to H^+ at lower ionic strength is consistent with the supposition that the pH dependence of Φ_{py} reflects the reaction of H^+ with another cationic species,[31] *e.g.*, A or CT_2*.

Other $Ru(NH_3)_5L^{2+}$ Complexes. The most striking features of the Φ_L values obtained for the complexes $Ru(NH_3)_5L^{2+}$ (Figure 2) is the pH insensitivity for L = benzonitrile and for L = 3-chloropyridine and the similarity of the data obtained for the 4-methylpyridine complex to that for the pyridine complex. Only in 2 M HCl does the 3-chloropyridine show a small enhancement (20–30%) of Φ_L while, within experimental uncertainty, Φ_L is unchanged for the benzonitrile complex. These observations are consistent with a step in the mechanism involving protonation of the ligand nitrogen atom. Benzonitrile, a very weak Brønsted base,[32] should be less susceptible to a protonation pathway as should 3-chloropyridine (pK_a = 2.8),[24] a weaker base than pyridine (pK_a = 5.3). As a result, the Φ_L *vs.* pH curve for the 3-chloropyridine complex should be shifted to lower pH while, in contrast, the complex of 4-methylpyridine (pK_a = 6.1)[24] should participate as well as the pyridine analog in a competitive acid-dependent step. These predictions are consistent with the data (Figures 1 and 2). Another interesting observation for the various pyridine complexes can be drawn from comparing values at which the quantum yields plateau in the higher pH range. These values follow the order ($\Phi_{(3\text{-chloropyridine})} > \Phi_{(\text{pyridine})} > \Phi_{(4\text{-methylpyridine})}$). This, incidentally, is opposite to that observed for the second-order rate constants [k(4-methylpyridine) > k(pyridine) > k(3-chloropyridine)] measured[24] for the thermal reaction of $Ru(NH_3)_5H_2O^{2+}$ with the various ligands to form the respective $Ru(NH_3)_5L^{2+}$ ions.

(31) R. P. Bell, "Acid-Base Catalysis," Oxford University Press, London, 1941, p 32.
(32) L. P. Hammett and A. J. Deyrup, *J. Amer. Chem. Soc.*, **54**, 4239 (1932).

Acknowledgments. This work was supported by the National Science Foundation (GP-26199), the Research Corporation, and the Petroleum Research Fund, administered by the American Chemical Society (4023-A3). We are indebted to Professors R. J. Watts and Henry Offen of University of California, Santa Barbara, for helpful discussion and the latter for the loan of certain equipment. The mass spectrometer used in the H/D exchange experiments was purchased with the help of the National Science Foundation (NSF-GP-8593).

Electron Transfer through Organic Structural Units. XI. Reductions of Pentaamminecobalt(III) Derivatives of Heterocyclic Bases with Chromium(II) and Europium(II)[1a]

Edward R. Dockal[1b] and Edwin S. Gould*

Contribution from the Department of Chemistry, Kent State University, Kent, Ohio. *Received June 14, 1971*

Abstract: The reductions, with Eu^{2+}, of 20 heterocyclic pentaamminecobalt(III) complexes, nine of them new, are compared to the corresponding Cr^{2+} reductions. In most cases the ratio of specific rates, $k_{Eu^{2+}}/k_{Cr^{2+}}$ (25°, μ = 1.3), lies in the range 8–25. Deviations from this pattern occur only with ligands having sites allowing reduction *via* remote attack; among such ligands are 4-carbethoxypyridine, methylated pyrazines, and 4-pyridone. In such instances, reduction with Cr^{2+} is strongly enhanced, but rate increases with Eu^{2+} are very slight. Spectra of solutions resulting from Cr^{2+} reduction of the pyrazine complexes indicate that the Cr(III) products are N-bonded to the pyrazine ring. Inner-sphere reduction by Eu^{2+}, if it occurs at all, is marginal in magnitude. The Cr^{2+} and Eu^{2+} reductions of the complex of *trans*-1,2-bis(4-pyridyl)ethylene (II) and the Eu^{2+} reduction of the 4-carbethoxypyridine derivative exhibit strong autocatalysis, suggesting intervention of an unusually reactive radical or radical cation. When $(NH_3)_5pyCo^{3+}$ is added to mixtures in which such autocatalytic reactions are occurring, it too is rapidly reduced. The suggestion is made that such reactive species operate through outer-sphere mechanisms.

The richness of the reactivity patterns observed in the Cr^{2+} reductions of organic $(NH_3)_5Co^{III}$ derivatives[2] has not yet been encountered with any other reducing center. Reductions with Cu^+, which is less strongly reducing than Cr^{2+} by 0.56 V, exhibit signs of the same mechanistic variations that come into play with Cr^{2+}, but the trends are less intense.[3] Moreover, rates of reductions with the still more poorly reducing Fe(II) are gathered at the very slow end of the kinetic scale.[4] On the other hand, reductions by the strongly

(1) (a) From the Ph.D. Dissertation of E. R. Dockal, Kent State University, 1971. This work was supported in part by the Petroleum Research Fund, administered by the American Chemical Society, under Grant 2878-A3. (b) NSF Trainee, 1969–1971.
(2) See, for example, H. Taube and E. S. Gould, *Accounts Chem. Res.*, **2**, 321 (1969).
(3) (a) O. J. Parker and J. H. Espenson, *J. Amer. Chem. Soc.*, **91**, 1968 (1969); (b) E. R. Dockal, E. T. Everhart, and E. S. Gould, *ibid.*, **93**, 5661 (1971).
(4) See, for example, J. H. Espenson, *Inorg. Chem.*, 4, 121 (1965).